

## STUDY ON RESIDUAL STRESS AND FRACTURE CHARACTERISTIC OF WELDED HIGH-DENSITY POLYETHYLENE PIPE

Laurentiu MUSAT \*, Teodor CARBUNARU\*, Veronica ARGESANU\*\*, Daniel TUNEA\*\*

\* DGN Buzau, itbz@distrigazsud.ro

\*\* Polytechnica University Timisoara, vargesanu@mec.utt.ro, dtunea@mec.utt.ro

### ABSTRACT

It is generally accepted that the non-homogeneity of flow and temperature gradients are the main causes of longitudinal and circumferential residual stress in pipe and welded high-density polyethylene pipe. The fracture characteristic of high-density polyethylene pipe for the supply of gaseous fuels subjected to welding process was studied at different temperature by the crack opening displacement (COD) method.

### 1. INTRODUCTION

It is generally accepted that the non-homogeneity of flow and temperature gradients are the main causes of residual stresses in extruded PEHD pipes. This state of stress in PEHD pipes is reported to be coupled with morphological variances [1, 6, 8]. At present, PEHD pipes are widely used for long term applications, especially in the transmission and distribution of natural gas and water. The evaluation of residual stresses in pipe and welded high density polyethylene becomes an important factor for the prediction of the long term failure of these PEHD pipes and their resistance to brittle crack propagation [3, 10].

### 2. RESIDUAL STRESS IN PEHD PIPES

The PEHD pipe pieces, each about 1m long, had a minimum wall thickness of 11,1mm and an average outside diameter of 113,7mm [2].

#### 2.1. LONGITUDINAL RESIDUAL STRESS

Estimation of the longitudinal residual stress component in the PEHD pipe sample considered is based on the method of TREUTING and READ [2]. This method has been employed for the evaluation of biaxial residual stress in plastic plates and circumferential residual stresses in PEHD pipes [2]. The technique involves removal of successive surface layers and measuring the resulting curvature. When the following three conditions are satisfied the accuracy of the method is limited only by the precision of the measurements [2]:

- ? the specimen is linear in pure bending for the range of curvature involved,
- ? the stress does not vary in the plane of the specimen but only through the thickness, and
- ? the removal of surface layers does not disturb the stress in the remaining material.

Thus, considering figure 2.1, the equation relating the curvature  $K$  to the residual stress  $\sigma_x$  is given by:

$$\sigma_x(z_1) = -\frac{E}{6(1-\nu^2)} \left\{ (z_0 + z_1)^2 \left[ \frac{d\kappa_x(z_1)}{dz_1} + \nu \frac{d\kappa_y(z_1)}{dz_1} \right] + 4(z_0 + z_1) [\kappa_x(z_1) + \nu\kappa_y(z_1)] - 2 \int_{z_1}^{z_0} [\kappa_x(z_1) + \nu\kappa_y(z_1)] dz \right\}$$

where  $E$  is Young's modulus and  $\nu$  is Poisson's ratio. The terms  $d\kappa/dz$  and  $\kappa dz$  have been evaluated graphically [2, 3, 5, 8].

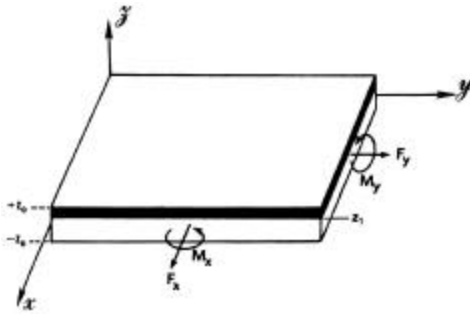


Figure 2.1. Schematic illustration of the development of forces and moments in a plate due to layer removal [2]

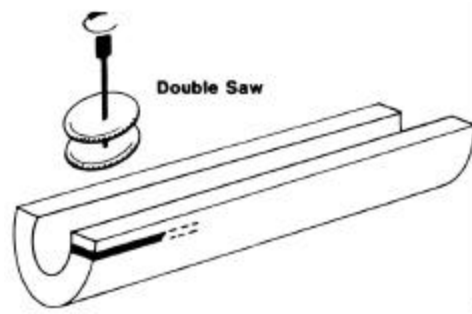


Figure 2.2. Double saw assembly for longitudinal strip specimen preparation [2].

The simulation of plates from hollow cylinders is achieved by cutting bars of rectangular cross section from the pipe wall. The specimens are prepared using an assembly of two identical circular saws with a thickness of 1.04 mm. The specimen width is set by spacers between the saws (figure 2.2). The cutting was performed on a Bridgeport milling machine at 325 rpm. The specimen and the saws were cooled with a stream of pressurized service air to minimize possible frictional heat generation. The dimensions of the specimens were 10 by 127 by 11.1 mm, where the last is the wall thickness of the pipe (figure 2.3) [6, 8].

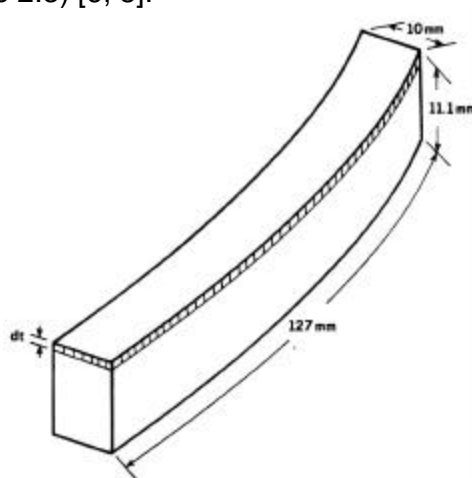


Figure 2.3. Sketch of the rectangular specimen as prepared [2].

Then the specimens were milled to one even level. Specimens with thicknesses of 3.70, 5.50, 10.20, and 11.10 mm were left to deform freely for one day [1, 2, 3, 5, 6]. The

resulting curvature after 24 h was measured graphically from which the longitudinal residual stress was deduced from the above equation (figure 2.4) [2, 5, 6]

## 2.2. CIRCUMFERENTIAL RESIDUAL STRESS

Evaluation of the residual stress component in the PEHD pipe sample considered is based on the method of RING SLITTING METHOD and STRAIN GAGE METHOD. A piece of PEHD pipe is turned using a lathe machine at a speed of 30 rpm. Two wooden mandrels were inserted into both ends of the PEHD pipe to provide rigidity. Three aluminum plates machined to the outside diameter of the pipe were inserted between the plastic and the lathe jaws to prevent tube damage [3, 5, 6, 8].

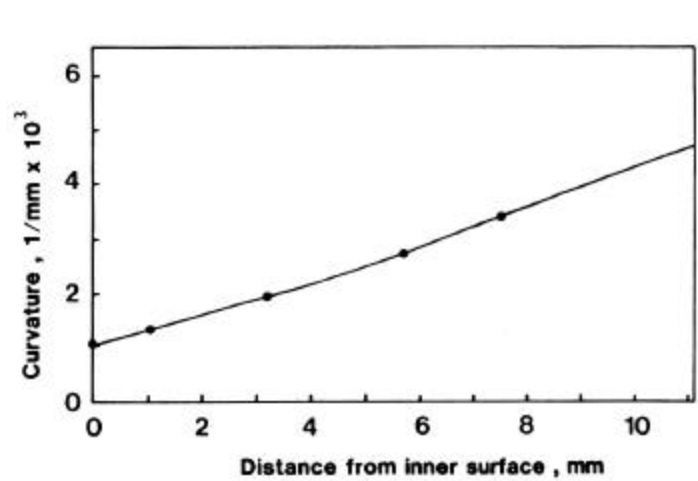


Figure 2.4. Curvature as a function of layer position (distance from inner pipe surface) [2].

At the other end the mandrel, shaped as a stopper, was aligned with a live center in the tailstock ram. When approaching the prescribed thickness, the cutting increment was reduced to 0.25 mm through the last millimetre. The rings were 15 mm wide. The turning was done with a 9.5 mm tool.

When neglecting the strain in the longitudinal direction, the proportionality relationship between the circumferential strain ( $\epsilon_{\theta}$ ) and the original diameter ( $d_0$ ) becomes  $\epsilon_{\theta} = \Delta d/d_0$  where  $\Delta d$  is the observed change in diameter from which the corresponding stress is computed. Diameter measurements were recorded 24 h after final sample preparation [2, 3, 5].

**STRAIN GAGE METHOD** —To obtain the strain distribution within the PEHD pipe wall, the strain gage technique, like all other methods, involves material removal. Perhaps its main advantage is that the strain in a given direction is readily measurable. In the case of PEHD pipes, it is assumed that the three principal stresses have a rotational symmetry along the longitudinal direction and around the cylinder axis [2, 3].

Rings 20 mm wide are prepared as described in the previous section, were adhered to the outer surface of the rings. General purpose strain gages were chosen. They are self-temperature compensated form and have a tough and flexible polyimide backing.

The strain gage was placed on the outer surface of the PEHD pipe ring, then the ring was cut into two halves so that the gage remained in a central location. For the innermost ring two gages were placed on both sides to obtain the residual strain at the bore. The half rings were left to deform for 24 h before recording the levels of residual strain. Residual stresses were calculated from strain measurements using a Young's modulus of  $0.56 \text{ GN m}^{-2}$  [2, 3].

The longitudinal residual stress ( $\sigma_z$ ) distribution obtained from curvature measurements using the layer removal method is shown in figure 2.5 (solid curve). Neglecting the radial stress component in the strip, the circumferential stress ( $\sigma_\theta$ ) distribution is obtained from the relationship  $\sigma_\theta = \nu \sigma_z$ , where  $\nu$  is Poisson's ratio. Taking  $\nu = 0.4$ , the circumferential stress distribution is shown by the broken curve in figure 2.5. This, of course, assumes linear elastic behavior. At the outer surface, the stresses are compressive with a maximum value of  $\sigma_z = 9.7 \text{ MN m}^{-2}$  and  $\sigma_\theta = 3.9 \text{ MN m}^{-2}$ . On the other hand, the innermost residual stresses are  $\sigma_z = 6.6 \text{ MN m}^{-2}$  and  $\sigma_\theta = 2.6 \text{ MN m}^{-2}$  in tension. The tensile residual stress dominates over about 24% of the wall thickness from the bore, at which thickness it gradually vanishes to become compressive. From figure 2.5 it is also obvious that none of the stress distributions satisfies equilibrium conditions.

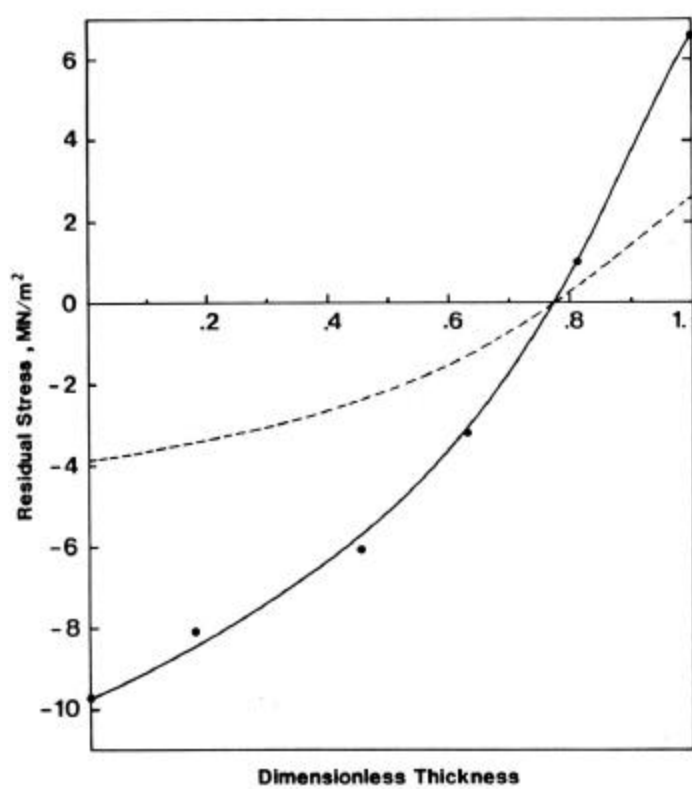


*Figure 2.5. Longitudinal residual stress distribution derived from curvature measurements. The broken curve represents the computed circumferential distribution [2].*

Residual stress obtained from ring closure measurements using the ring slitting method is depicted in figure 2.6 (solid curve). The broken curve represents the longitudinal stress distribution computed as indicated earlier. These results are qualitatively similar to those reported in figure 2.5. Essentially, the residual stress is compressive at the outer surface of the PEHD pipe wall and tensile at its bore. The magnitude of the maximum tensile residual stresses ( $\sigma_z$  and  $\sigma_\theta$ ) reported here are approximately similar to those reported in figure 2.5. Nevertheless, the maximum residual compressive stresses are about twofold the values obtained from longitudinal layer removal method of figure 2.6. It also appears that tensile residual stresses dominate much deeper into the pipe wall (~30% compared to 24% of the wall thickness).

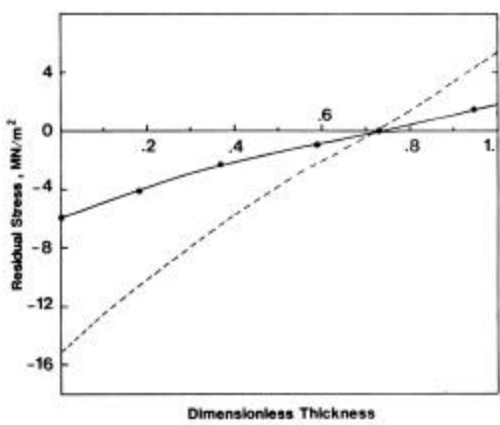


Figure 2.6. Circumferential residual stress distribution derived from ring closure measurements. The broken curve is the computed longitudinal component.

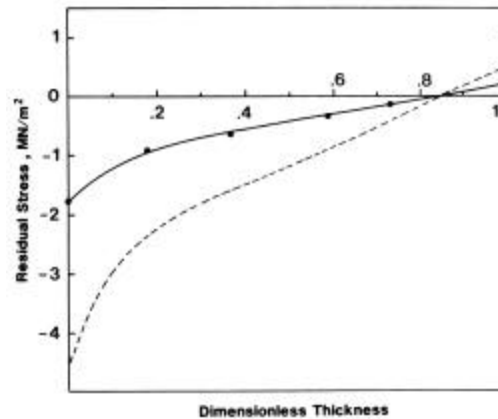


Figure 2.7. Circumferential stress distribution obtained from direct strain measurements. The broken curve represents the computed values of the longitudinal component.

In order to discover whether more realistic values can be obtained, strain gage measurements were carried out as outlined earlier. The results are displayed in figure 2.7 for circumferential (solid curve) and longitudinal (broken curve) residual stresses. As previously indicated, the residual stresses are compressive outside and tensile at the bore vanishing at about 20% from the bore. However, the stresses are much lower than those obtained from the previous techniques. This is illustrated by the summary of the maximum residual stresses obtained from figures 2.5, 2.6, and 2.7, and presented in table 2.1.

Residual stress assessment in a great many plastic components, particularly if the material is not transparent, is only accessible through techniques involving layer removal. Hence these results ought to be considered in light of the limitations inherent in such measurements [3, 5, 6, 8].

As alluded to earlier, the analysis is based on three assumptions:

- ? linearity of the sample in pure bending,
- ? constancy of the stress within the plane of the strip, and
- ? removal of layers does not disturb the stress state of the remaining material.

Table 2.1. Comparison of the maximum values of the residual stress along the longitudinal ( $a_z$ ) and circumferential ( $a_\theta$ ) directions obtained from the different methods employed [2].

Method	$\sigma_\theta^{IN}$ (MN m <sup>-2</sup> )	$\sigma_\theta^{OUT}$ (MN m <sup>-2</sup> )	$\sigma_z^{IN}$ (MN m <sup>-2</sup> )	$\sigma_z^{OUT}$ (MN m <sup>-2</sup> )
Modified LR	2.6	-3.9	+ 6.6"	-9.7"
Ring Slitting	1.8"	-6.0"	4.5	-15.0
Strain Gage	0.2"	-1.8"	0.5	-4.5

"These values are derived from residual strain measurements; the others are computed from  $\sigma_\theta = \sigma_z$ .

In addition, residual stresses are naturally coupled with, or an actual manifestation of, microstructural gradients. In polyethylene pipes, these microstructural gradients may well result in different "elastic" properties which could impose additional limitations.

However, in spite of all the limitations, assessment of residual stresses constitutes a significant design consideration in long term applications [2, 3, 5, 8].

The results obtained from strain gage measurements (figure 2.7) appear more realistic. The residual stress value obtained from strain gage measurements gives rise to a net tensile force in the notch tip field to allow its propagation. Hence the energy release rate along the crack trajectory was calculated from the longitudinal residual stress distribution of figure 2.7. Otherwise, the data from curvature measurements, if employed, would predict crack propagation within a compressive stress field which is unrealistic.

It is important that the achievement of a practical stress distribution by means of the strain gage technique should not draw our attention from the need to examine several unresolved limitations. These include the effect of localized heating on adhesion and sensitivity of the gages, material nonlinearity, structural changes induced by layer removal, and possible nonuniformity of elastic properties across the PEHD pipe wall.

### 3. FRACTURE CHARACTERISTIC OF WELDED HIGH DENSITY POLYETHYLENE PIPE

In [4] the fracture behaviour of PEHD for the supply of gaseous fuels and its butt-fusion joint were studied at different testing temperature of  $-78^{\circ}\text{C}$ ,  $-40^{\circ}\text{C}$ ,  $-20^{\circ}\text{C}$ ,  $0^{\circ}\text{C}$  and  $20^{\circ}\text{C}$ , by means of the crack opening displacement method and the critical value  $\delta_{is}$  of COD techniques.

The sketch of butt-fusion welded joint is shown in figure 3.1.

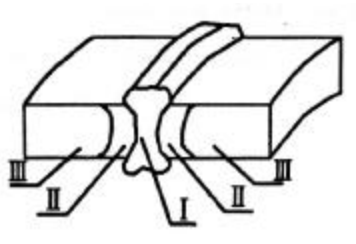


**Figure 3.1. The sketch of butt-fusion welded joint of PEHD;**  
**I - fusion zone; n - heat affected zone; m - base pipe material**

Bars of dimensions 19 mm x 38 mm x 180 mm, used as single-edge notch specimen (figure 3.2) for fracture test, were machined from PEHD pipe directly. Notching was performed in two steps; first a notch of 15 mm depth was cut by the disc saw, and then additional 4 mm at the tip of the notch was made by a sharp V-blade of radius not more than 25  $\mu\text{m}$ , and a notch length (a) to specimen width (W) ratio of 0.5 are kept. This procedure saves time and minimizes wear of the V-blade, while producing a sufficiently sharp for fracture testing [4, 5, 7, 8, 9, 10].

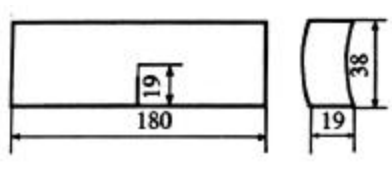


**Figure 3.2. Three point bend specimen with pre-crack**

The various zones of the PEHD welded joint, which were studied, are shown in figure 3.1. The weld is divided into two zones: the fusion zone and heat affected zone (I, II

respectively in figure 3.1). Notches were cut at different zones shown in figure 3.1. respectively [4].

Testing results at different temperature are shown in figure 3.3. They show that as the test temperature is lowered, saturation initial crack COD  $\delta_{i5}$  of every zone such as PEHD pipe material, fusion zone and heat affected zone decrease. As the test temperature is lowered, stiffness of PEHD pipes materials increased rapidly. The influence of testing temperature on fracture characteristic is due to the greater increasing of material stiffness with temperature decreasing. As the temperature is lowered, the materials maintain a higher load carrying capacity due to the greater increase in stiffness. However, its energy absorbing capacity is decreased as fracture become unstable. For example its load carrying capacity at 20°C is 1.2 kN, but at -78°C its load carrying capacity is 2.3 kN. Tensile test at different temperature has shown the same results [4].  $\delta_{i5}$  is larger than 0.4 at 20°C, but almost to zero at -78°C.

The change of mode of fracture at different temperature is also verified by the examination of the fracture surface (figure 3.4). The fracture surface shows the characteristic dimple-type profile of a ductile tearing mode. As the test temperature is lowered, the size of the dimples becomes smaller, at the same time the depth of the dimples also becomes smaller, reflecting the decrease in ductility on micro-level. All the test specimens in this test fail in ductile tearing [4, 5, 8, 9, 10].

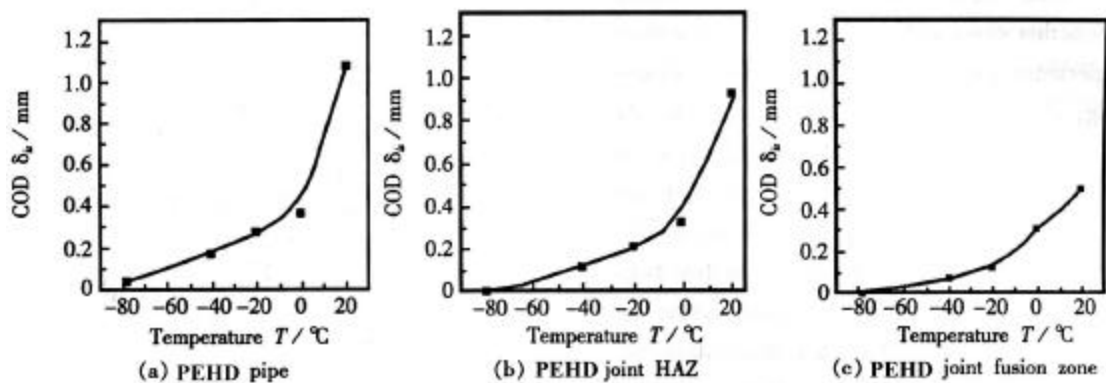


Figure 3.3. Saturation initiation crack COD  $\delta_{56}$  at different temperature [4]

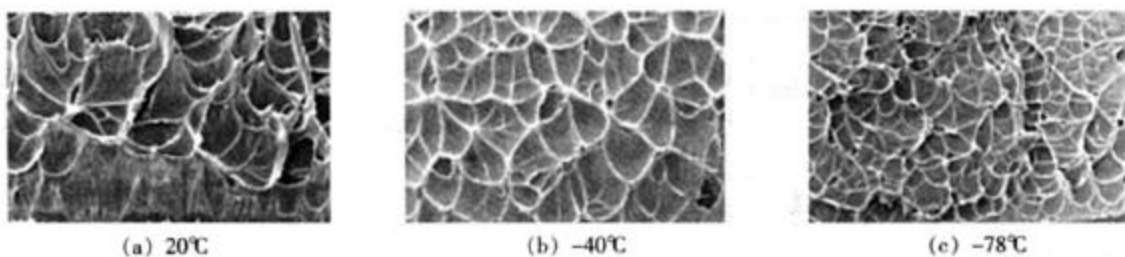


Figure 3.4. SEM of fusion zone of HOPE butt-joint fracture surface [4]

The crack extension  $\Delta a$  was examined after three point bend test. The same phenomenon was found. As the test temperature is lowered, the crack extension  $\Delta a$  becomes larger, reflecting the decrease in crack extension resistance, and crack opening displacement becomes smaller as the test temperature is lowered. On the other hand the mode of fracture becomes unstable [4].

#### 4. CONCLUSIONS

4.1. The non-homogeneity of flow and temperature gradients are the main causes of residual stresses in pipe and welded high density polyethylene pipe.

4.2. Estimation of the longitudinal residual stress component in the PEHD pipe sample considered is based on the method of TREUTING and READ; estimation of the circumferential residual stress in PEHD pipe sample considered on the method of RING SLITTING METHOD and STRAIN GAGE METHOD.

4.3. The fracture behaviour of PEHD for butt-fusion joint were studied at different testing temperature by means of the crack opening displacement method and the critical value  $\sigma_{is}$  of COD techniques. The influence of testing temperature on fracture characteristic is due to the greater increasing of material stiffness with temperature decreasing.

#### BIBLIOGRAPHY

- [1]. CALVERT, G. and co.: The use of thermoplastic stress analysis to identify defects in polymeric materials, INSIGH, 2004, vol. 46, nr. 9, p. 550-553
- [2]. CHAOUI, K. and co: Strain Gage Analysis of Residual Stress in Plastic Pipes, JOURNAL of TESTING and EVALUATION, 1988, nr. 2, p. 286-290
- [3]. ESAULENKO, G.B. and KONDRATENKO, V.Yu.: Study of strength characteristics of polyethylene butt welded joints and development of testing methods, DOC IIS/IIW-XVI-584-90
- [4]. FANGJUAN, Qi s.a.: Study on fracture characteristic of welded high-density polyethylene pipe, CHINA WELDING, 2002, vol. 11, nr. 1, p. 59-63
- [5]. HASHEMI, S. and WILLIAMS, J.G.: Fracture characteristic of trough polymers using J method, Polymer Engineering and Science, 1986, vol. 26, nr. 11, p. 761-767
- [6]. MANDEL, J.F. and co.: Plane strain fracture toughness of polyethylene pipe materials, POLYMER ENGINEERING AND SCIENCE, 1983, vol. 23, nr. 7, p. 404-411
- [7]. NIELSEN, L.E.: Mechanical properties of polymers and composites, Edition MARCEL DEKKER, New York, 1994, USA
- [8]. POPESCU, M.: Tehnici de îmbinarea materialelor plastice, Editura POLITEHNICA, Bucuresti, 2004
- [9]. WILLIAMS, J.G.: Fracture mechanics of polymers, Chichester Ellis Harwood Limited, 1984, USA
- [10]. YUCHUAN, Z.: Developing prospects of polyethylene pipe, CHINA PLASTIC, 1999, vol. 13, nr. 2, p. 21-26